Handling Imbalance Between Convergence and Diversity in the Decision Space in Evolutionary Multi-Modal Multi-Objective Optimization *Supplementary Material*

Yiping Liu, *Member, IEEE*, Hisao Ishibuchi, *Fellow, IEEE*, Gary G. Yen, *Fellow, IEEE*, Yusuke Nojima, *Member, IEEE*, and Naoki Masuyama, *Member, IEEE*

***Abstract*—This is the supplementary material for Handling Imbalance Between Convergence and Diversity in the Decision Space in Evolutionary Multi-Modal Multi-Objective Optimization. This supplementary material provides the investigations on (1) the property of some existing MMOPs and (2) the behavior of CPDEA.**

I. Investigation on the Property of MMMOP1, Omni-Test Problem, and SYM-PART

In this section, we investigate the property of MMMOP1 [1], Omin-test problem [2], and SYM-PART [3] with two objectives and two decision variables. In SYM-PART, a, b, c are set to 0.1, 1, 0.8, respectively.

MMMOP1 has five equivalent Pareto optimal subsets. Omni-test problem and SYM-PART have nine equivalent Pareto optimal subsets. They are listed in Table I.

In Fig. 1, we show the fitness landscape based on Pareto rank of these problems, where each line segment is an equivalent Pareto optimal subset of the corresponding problem. We can see from Fig. 1 that for each problem, the pattern around each equivalent Pareto optimal subset is the same. This implies that the difficulties in finding equivalent Pareto optimal subsets are the same.

To check whether these problems meet the first condition in Definition 2, Fig. 2 shows the average Pareto rank of solutions close to each equivalent Pareto optimal subset, where S_i ($i = 1, \ldots, 5$ for MMMOP1, and $i = 1, \ldots, 9$ for Omni-test problem and SYM-PART) is the set of solutions whose distances to the ith equivalent Pareto optimal subset are smaller than d_{th}. We can see from Fig. 2 that for each problem, the average Pareto rank of solutions close to each equivalent Pareto optimal subset is the same. Therefore, these problem do not satisfy the first condition.

To check the second condition, in Fig. 3, for each problem, we show the results of IGDX over 40 runs when DNEA was used to solve some new optimization problems, MOPi ($i = 1, \ldots, 5$ for MMMOP1, and $i = 1, \ldots, 9$ for Omni-test problem and SYM-PART). The objective functions of MOPi are the same to those of the original MMOP (i.e., MMMOP1, Omni-test problem, or SYM-PART). The bounds of x_1 and x_2 in each MOP are listed in Table I. The PS of MOPi is the same to the ith equivalent Pareto optimal subset of the corresponding MMOP. We can see from Fig. 3 that for each problem, the curves of IGDX when solving these MOPs are almost the same. Therefore, the complexities of searching for the equivalent Pareto optimal subsets are the same, and the second condition is not met.

Based on the above results, we can see that MMMOP1, Omni-test problem, and SYM-PART are not MMOP-ICDs. The property of other MMOPs can be investigated in the same way, and most existing benchmark MMOPs are not MMOP-ICDs.

II. Further Investigations on the Behavior of CPDEA

We investigate two key parameters, η and p, to observe their effects on the behavior of CPDEA and thus to provide guidelines for setting them. We show the results of CPDEA on IDMP-M2-T1. Similar results were obtained on other test problems while they are not shown here. In addition, we visualize the final population of CPDEA on different test problems for an intuitive understanding of the CPD method.

A. Sensitivity Analysis of η

We applied CPDEA to IDMP-M2-T1 with different settings of η ($\eta = 1, \ldots, 10$). The average IGDX and IGDM values over 40 runs are shown in Fig. 4. Note that p is set to 1 to avoid using the second reproduction operator. We can see from Fig. 4

This work was supported in part by the National Natural Science Foundation of China under Grant 61876075 and Grant 61803192, in part by the Program for Guangdong Introducing Innovative and Enterpreneurial Teams under Grant 2017ZT07X386, in part by the Shenzhen Peacock Plan under Grant KQTD2016112514355531, in part by the Science and Technology Innovation Committee Foundation of Shenzhen under Grant ZDSYS201703031748284, in part by the Program for University Key Laboratory of Guangdong Province under Grant 2017KSYS008, and in part by Japan Society for the Promotion of Science (JSPS) KAKENHI under Grant JP19K20358. (*Corresponding Author: Hisao Ishibuchi*)

Y. Liu, Y. Nojima, and N. Masuyama are with Department of Computer Science and Intelligent Systems, Graduate School of Engineering, Osaka Prefecture University, Sakai, Osaka 599-8531, Japan. (yiping0liu@gmail.com, nojima@cs.osakafu-u.ac.jp, masuyama@cs.osakafu-u.ac.jp)

H. Ishibuchi is with Shenzhen Key Laboratory of Computational Intelligence, University Key Laboratory of Evolving Intelligent Systems of Guangdong Province, Department of Computer Science and Engineering, Southern University of Science and Technology, Shenzhen 518055, China. (hisao@sustech.edu.cn)

G. G. Yen is with the School of Electrical and Computer Engineering, Oklahoma State University, Stillwater, OK 74078, USA. (gyen@okstate.edu)

TABLE I
THE EQUIVALENT PARETO OPTIMAL SUBSETS OF MMMOP1, OMNI-TEST PROBLEM, AND SYM-PART. THE BOUNDS OF x_1 AND x_2 IN THE OPTIMIZATION PROBLEM, MOPi, WHOSE PS IS THE SAME TO THE CORRESPONDING EQUIVALENT PARETO OPTIMAL SUBSET.

	MMMOP1			Omni-test problem			SYM-PART		
i	i th equivalent Pareto optimal subset	Bound of x_1 in MOPi	Bound of x_2 in MOPi	i th equivalent Pareto optimal subset	Bound of x_1 in MOPi	Bound of x_2 in MOPi	i th equivalent Pareto optimal subset	Bound of x_1 in MOPi	Bound of x_2 in MOPi
1	$x_2 = 0.1$	[0, 1]	[0, 0.2]	$x_1 = x_2, x_1 \in [1, 1.5]$	[0, 2]	[0, 2]	$x_2 = -1, x_1 \in [-1.1, -0.9]$	[-1.5, -0.5]	[-1.5, -0.5]
2	$x_2 = 0.3$	[0, 1]	[0.2, 0.4]	$x_1 = x_2 + 2, x_1 \in [3, 3.5]$	[2, 4]	[0, 2]	$x_2 = -1, x_1 \in [-0.1, 0.1]$	[-0.5, 0.5]	[-1.5, -0.5]
3	$x_2 = 0.5$	[0, 1]	[0.4, 0.6]	$x_1 = x_2 + 4, x_1 \in [5, 5.5]$	[4, 6]	[0, 2]	$x_2 = -1, x_1 \in [0.9, 1.1]$	[0.5, 1.5]	[-1.5, -0.5]
4	$x_2 = 0.7$	[0, 1]	[0.6, 0.8]	$x_1 = x_2 + 2, x_1 \in [1, 1.5]$	[0, 2]	[2, 4]	$x_2 = 0, x_1 \in [-1.1, -0.9]$	[-1.5, -0.5]	[-0.5, 0.5]
5	$x_2 = 0.9$	[0, 1]	[0.8, 1]	$x_1 = x_2, x_1 \in [3, 3.5]$	[2, 4]	[2, 4]	$x_2 = 0, x_1 \in [-0.1, 0.1]$	[-0.5, 0.5]	[-0.5, 0.5]
6	\	\	\	$x_1 = x_2 - 2, x_1 \in [5, 5.5]$	[4, 6]	[2, 4]	$x_2 = 0, x_1 \in [0.9, 1.1]$	[0.5, 1.5]	[-0.5, 0.5]
7	\	\	\	$x_1 = x_2 + 4, x_1 \in [1, 1.5]$	[0, 2]	[4, 6]	$x_2 = 1, x_1 \in [-1.1, -0.9]$	[-1.5, -0.5]	[0.5, 1.5]
8	\	\	\	$x_1 = x_2 + 2, x_1 \in [3, 3.5]$	[2, 4]	[4, 6]	$x_2 = 1, x_1 \in [-0.1, 0.1]$	[-0.5, 0.5]	[0.5, 1.5]
9	\	\	\	$x_1 = x_2, x_1 \in [5, 5.5]$	[4, 6]	[4, 6]	$x_2 = 1, x_1 \in [0.9, 1.1]$	[0.5, 1.5]	[0.5, 1.5]

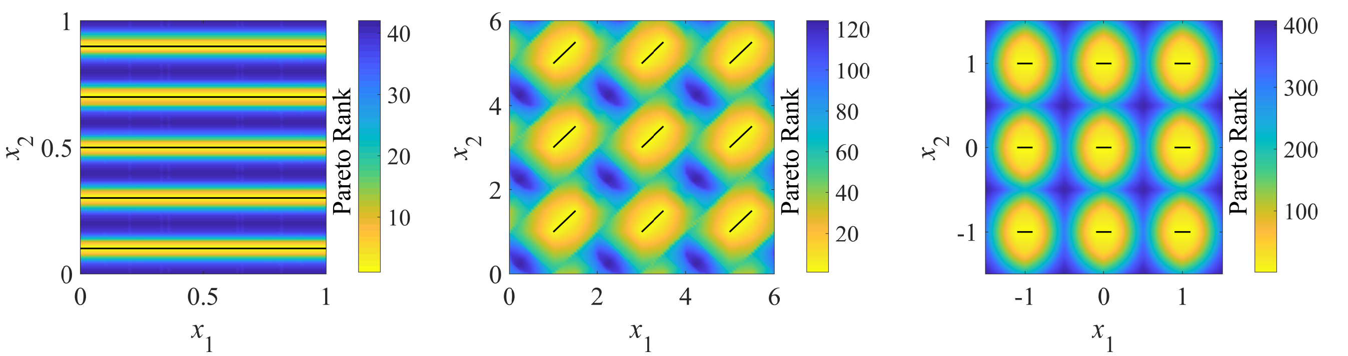

(a) MMMOP1 (b) Omin-test problem (c) SYM-PART

Fig. 1. The fitness landscapes based on Pareto rank of MMMOP1, Omin-test problem, and SYM-PART. For each problem, $10,201$ (101×101) solutions are uniformly sampled in the entire decision space. They are in different colors based on their Pareto ranks. A brighter (warmer) tone corresponds to a lower Pareto rank. Each line segment is an equivalent Pareto optimal subset.

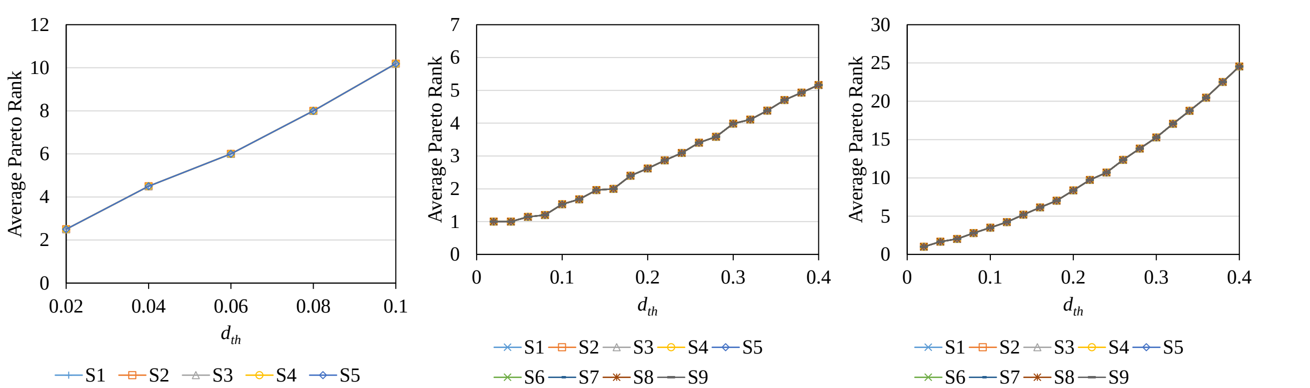

(a) MMMOP1 (b) Omin-test problem (c) SYM-PART

Fig. 2. The average Pareto rank of solutions close to each equivalent Pareto optimal subset based on Fig. 1. S_i ($i = 1, \ldots, 5$ for MMMOP1, and $i = 1, \ldots, 9$ for Omni-test problem and SYM-PART) is the solutions whose distances to the ith equivalent Pareto optimal subset is smaller than d_{th}.

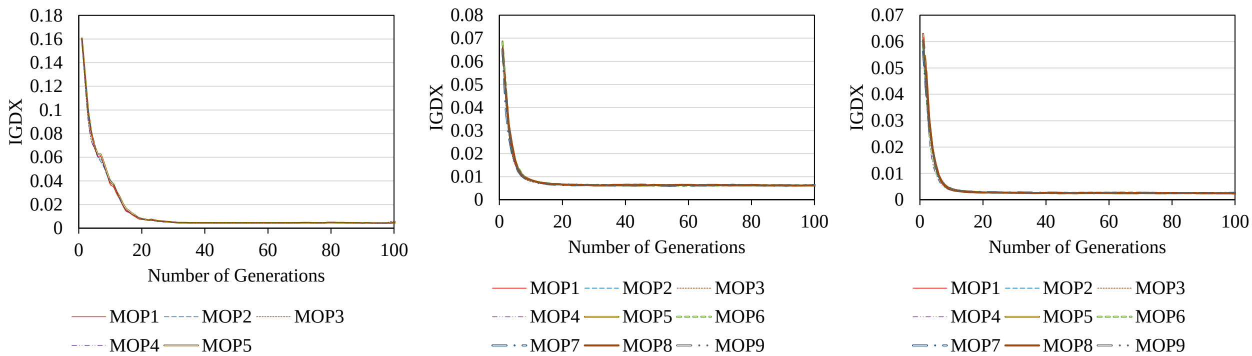

(a) MMMOP1 (b) Omin-test problem (c) SYM-PART

Fig. 3. The IGDX value (averaged over 40 runs) with respect to generations when using DNEA to some new optimization problems.

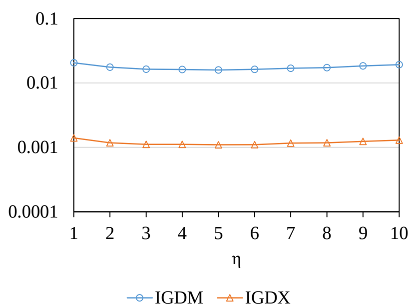

Fig. 4. The average IGDX and IGDM values over 40 runs obtained by CPDEA on IDMP-M2-T1 with different settings of η.

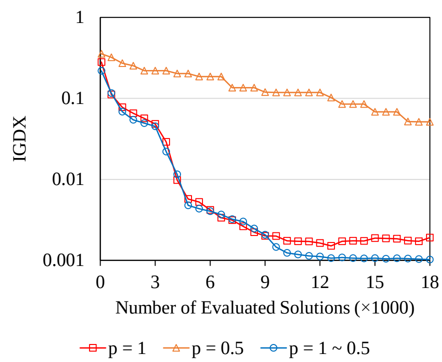

Fig. 5. The average IGDX value over 40 runs with respect to the number of evaluate solutions obtained by CPDEA on IDMP-M2-T1 with $\alpha = 10$.

that all the IGDX and IGDM values under different settings of η are quite good, and the differences among the IGDX (or IGDM) values are very small. This means that CPDEA shows a robust performance under different settings of η.

B. Sensitivity Analysis of p

We used IDMP-M2-T1 with $\alpha = 10$ to investigate the effect of p. We set α to such a large value to increase the difficulty in finding EPS2, so that the effect of p can be easily observed. In Fig. 5, we show the average IGDX value over 40 runs with respect to the number of evaluated solutions, which were obtained by CPDEA with different settings of p, i.e., $p = 1$, 0.5, and $1 \sim 0.5$. $p = 1 \sim 0.5$ means that we set $p = 1$ before the number of evaluated solutions reached $9,000$ and $p = 0.5$ after that. We can see from Fig. 5 that when $p = 0.5$ through the entire evolution, the convergence rate according to IGDX is much slower than the case of $p = 0$. We also observed that (which are not shown here) almost no solution close to EPS2 had been found by setting $p = 0.5$. This indicates that executing the second reproduction operator will reduce the efficiency of searching for an EPS when no solution close to it has been found. When $p = 1$, the solutions close to each EPS had been found before the number of evaluated solutions reached $9,000$. Then changing p to 0.5 further decreased the IGDX value. This suggests that the second reproduction operator can enhance the algorithm's exploitation ability under such a situation. Note that for different optimization problems, the difficultly in finding each EPS is different. Therefore, it may be needed to develop a method to adaptively tune p, which is an interesting future research topic.

C. Visualization of the Final Population of CPDEA

Fig. 6 shows the final population of DNEA on two-objective IDMPs, IDMP-M3-T1 and IDMP-M4-T1, in a single run. This particular run is associated with the result which is the closest to the mean IGDX value in Table III in the main body of the paper. The results on three- and four-objective IDMPs in Types 2, 3, and 4 are similar to those in Type1. We can see from Fig. 6 that the solutions are dense in the regions where the EPSs locate and sparse in the other regions. It is interesting to note that the patterns of solutions in Fig. 6 (a)-(d) are similar to the corresponding fitness landscapes in Fig. 3 in the main body of the paper.

References

[1] Y. Liu, G. G. Yen, and D. Gong, "A multi-modal multi-objective evolutionary algorithm using two-archive and recombination strategies," *IEEE Transactions on Evolutionary Computation*, vol. 23, no. 4, pp. 660–674, 2019.

[2] K. Deb and S. Tiwari, "Omni-optimizer: A generic evolutionary algorithm for single and multi-objective optimization," *European Journal of Operational Research*, vol. 185, no. 3, pp. 1062–1087, 2008.

[3] G. Rudolph, B. Naujoks, and M. Preuss, "Capabilities of EMOA to detect and preserve equivalent pareto subsets," in *International Conference on Evolutionary Multi-Criterion Optimization*. Springer, 2007, pp. 36–50.

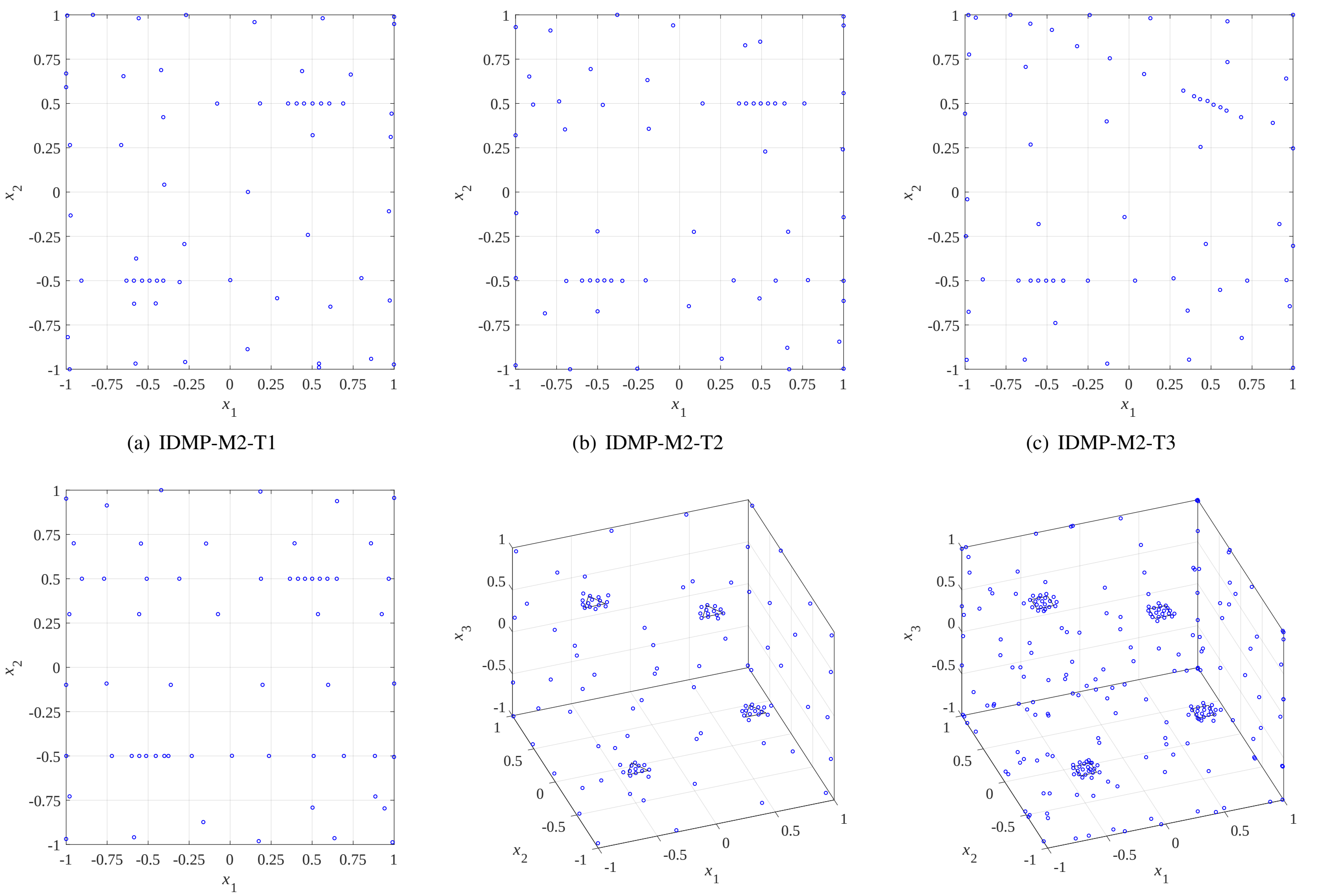

(a) IDMP-M2-T1 (b) IDMP-M2-T2 (c) IDMP-M2-T3

(d) IDMP-M2-T4 (e) IDMP-M3-T1 (f) IDMP-M4-T1

Fig. 6. The final population of DNEA on different test problems in a single run. This particular run is associated with the result which is the closest to the mean IGDX value in Table III in the main body of the paper.